

Two-body electrodisintegration of nuclei with antisymmetrized molecular dynamics

G J Rampho¹, S A Sofianos¹, S Oryu²

¹ Department of Physics, University of South Africa, Pretoria 0003, South Africa

² Department of Physics, Tokyo University of Science, Noda, Chiba 278-8510, Japan

E-mail: ramphogj@gmail.com

Abstract. Electron-induced proton knock-out process from the ${}^4\text{He}$ nucleus is investigated. Bound states of the systems are described with the angular-momentum-projected and parity-projected antisymmetrized molecular dynamics wave functions. The nuclear Hamiltonian is constructed with a semi-realistic nucleon-nucleon potential. Non-relativistic nuclear charge and current operators are employed in calculating nuclear transition amplitudes. Final-state interactions are taken into account by the use of the Glauber approximation. It is found that the antisymmetrized molecular dynamics generates a very good description of experimental data at high momentum transfer.

1. Introduction

Quasielastic electron-nucleon scattering is a very useful tool to extract important information about nuclear structure [1]. This is based on the fact that the interaction of the electrons and nuclei is predominantly electromagnetic and the theory underlying electromagnetic interactions, quantum electrodynamics theory, is well understood. Furthermore, the electromagnetic interactions are a lot weaker than nuclear interactions, and thus can be treated as a small perturbation to the nuclear Hamiltonian. Therefore, only one-photon exchange processes are dominant. In the one-photon approximation the electron and nuclear structure functions factor out completely in the transition form factor. Therefore, the only input quantities requiring careful construction are the nuclear wave functions. In this work the antisymmetrized molecular dynamics (AMD) to construct wave functions for bound nuclear systems to study proton knock-out process ${}^4\text{He}(e, e' p){}^3\text{H}$.

The AMD approach was developed [2] from the Time-Dependent Cluster Model [3] for the study of fermionic systems. This approach combines Fermi-Dirac statistics with elementary quantum mechanics to treat the motion of particles in a system [4]. However, the model is not fully quantum mechanical and does not assume a shell structure for the system. The AMD approach was used to study the dynamics of heavy-ion collisions [5] and elastic proton-nucleus scattering [6]. Clustering in nuclei as well as angular distributions of scattered protons in proton-nucleus scattering can be explained by the AMD model [6]. Improved AMD wave functions have been shown to give satisfactory predictions of properties of few-body systems [7, 8]. In this work we use the parity-projected and angular-momentum-projected AMD [9].

In Section 2 key features of the AMD approach are summarized. In this section the construction of the wave function, the equations of motion of the variable parameters and the

variational technique used are briefly outlined. Basic features of the electron-nucleus scattering formalism are given in Section 3. In Section 4 the theoretical results are compared with some experimental data for the proton knock-out from the ${}^4\text{He}$ nucleus. Conclusions drawn are indicated in Section 5.

2. AMD Formalism

An AMD wave function describing a bound nuclear system of A nucleons is constructed as a Slater determinant

$$\Psi_{AMD}(\vec{S}) = \frac{1}{\sqrt{A!}} \det[\phi_j(\alpha, \vec{s}_i), \chi_j(\vec{\sigma}_i), \xi_j(\vec{\tau}_i)] \quad (1)$$

where ϕ , χ and ξ are, respectively, the spatial, spin and isospin components of the single-particle wave functions. A wave function with definite parity (π) and total angular momentum (J), with total angular momentum projection (M) onto the quantization axis, is constructed from the AMD wave function as

$$\Psi_{MK}^{J\pi}(\vec{S}) = \frac{1}{2} P_{MK}^J(\Omega) [1 \pm P^\pi] \Psi_{AMD}(\vec{S}) \quad (2)$$

where $P_{MK}^J(\Omega)$ is the angular momentum projection operator, P^π the parity projection operator and $\vec{S} \equiv \{\vec{s}_1, \vec{s}_2, \vec{s}_3, \dots, \vec{s}_A\}$. The angular momentum projection operator is defined by [10]

$$P_{MK}^J(\Omega) = \frac{2J+1}{8\pi^2} \int d\Omega D_{MK}^{J*}(\Omega) \hat{R}(\Omega) \quad (3)$$

where $D_{MK}^J(\Omega)$ is the Wigner D -function, $\hat{R}(\Omega)$ the rotation operator and $\Omega \equiv \{\alpha, \beta, \gamma\}$ the Euler rotation angles.

The single nucleon wave functions are given by

$$\psi_i(\vec{r}_j) = \left(\frac{2\alpha}{\pi}\right)^{2/4} \exp\left[-\alpha\left(\vec{r}_j - \frac{\vec{s}_i(t)}{\sqrt{\alpha}}\right)^2 + \frac{1}{2}\vec{s}_i^2(t)\right] \otimes \chi_i \otimes \xi_i \quad (4)$$

where $\chi_i \otimes \xi_i$ are time-independent spin-isospin states of the i -th nucleon. These states are compactly expressed in the form $\kappa_i = \{N\uparrow \text{ or } N\downarrow\}$ for nucleon with spin-up or spin-down. The Gaussian width parameter α is a real constant and the variational parameter $\vec{s}(t)$ is complex. The time-dependent variational principle [5]

$$\delta \int_{t_1}^{t_2} \frac{\langle \Psi(\vec{S}) | i\hbar \frac{\partial}{\partial t} - H | \Psi(\vec{S}) \rangle}{\langle \Psi(\vec{S}) | \Psi(\vec{S}) \rangle} dt = 0 \quad (5)$$

with the constraints

$$\delta\Psi(t_1) = \delta\Psi(t_2) = \delta\Psi^*(t_1) = \delta\Psi^*(t_2) = 0 \quad (6)$$

is used to determine the dynamical equations for the variational parameters. The resulting equations are solved to minimize the variational energy

$$E_0^{J\pm}(\vec{S}, \vec{S}^*) = \frac{\langle \Psi_{MK}^{J\pm}(\vec{S}) | H | \Psi_{MK}^{J\pm}(\vec{S}) \rangle}{\langle \Psi_{MK}^{J\pm}(\vec{S}) | \Psi_{MK}^{J\pm}(\vec{S}) \rangle} \quad (7)$$

of the nucleus and also determine the variational parameters. The Hamiltonian of the system is constructed with the AV4 NN potential including the $V_{C1}(r)$ Coulomb component [11]. The evaluation of the components of the energy expectation values is explained in Ref. [12, 13].

The wave function describing a nucleon separation from a nucleus is written in the form [13]

$$\Psi_{\vec{S}}(\vec{r}_1, \vec{r}_2, \dots, \vec{r}_A) = \frac{1}{\sqrt{A!}} \begin{vmatrix} \psi_1(\vec{r}_1) & \psi_2(\vec{r}_1) & \cdots & G(\vec{R}) \bar{\psi}_A(\vec{r}_1) \\ \psi_1(\vec{r}_2) & \psi_2(\vec{r}_2) & \cdots & G(\vec{R}) \bar{\psi}_A(\vec{r}_2) \\ \vdots & \vdots & \ddots & \vdots \\ \psi_1(\vec{r}_A) & \psi_2(\vec{r}_A) & \cdots & G(\vec{R}) \bar{\psi}_A(\vec{r}_A) \end{vmatrix} \quad (8)$$

where nucleon A is the one ejected, \vec{r}_i the position vector of the i -th nucleon and $\bar{\psi}_A(\vec{r})$ a plane wave. The $G(\vec{R})$ is the Glauber multiple-scattering operator which approximates the final state interaction (FSI). This operator is given by [14]

$$G(\vec{R}) = \prod_{j=1}^{A-1} \left[1 - \Gamma(\vec{b}_A - \vec{b}_j) \theta(z_j - z_A) \right] \quad (9)$$

where $\theta(z)$ is the step function and $\Gamma(\vec{b})$ the nucleon-nucleon scattering profile function. The profile function is given by

$$\Gamma(\vec{b}) = \frac{\sigma_{NN}(1 - i\epsilon_{NN})}{4\pi \beta_{NN}^2} \exp \left[-\frac{b^2}{2\beta_{NN}^2} \right]. \quad (10)$$

where the vector \vec{B} is defined through the notation $\vec{r}_n = \vec{b}_n + \hat{q}z_n$. The parameters σ_{NN} , ϵ_{NN} and β_{NN} are determined by fitting $\Gamma(\vec{b})$ to nucleon-nucleon scattering experimental data at some invariant energy. The first three terms of the Glauber operator considered in this work are illustrated in figure 1.

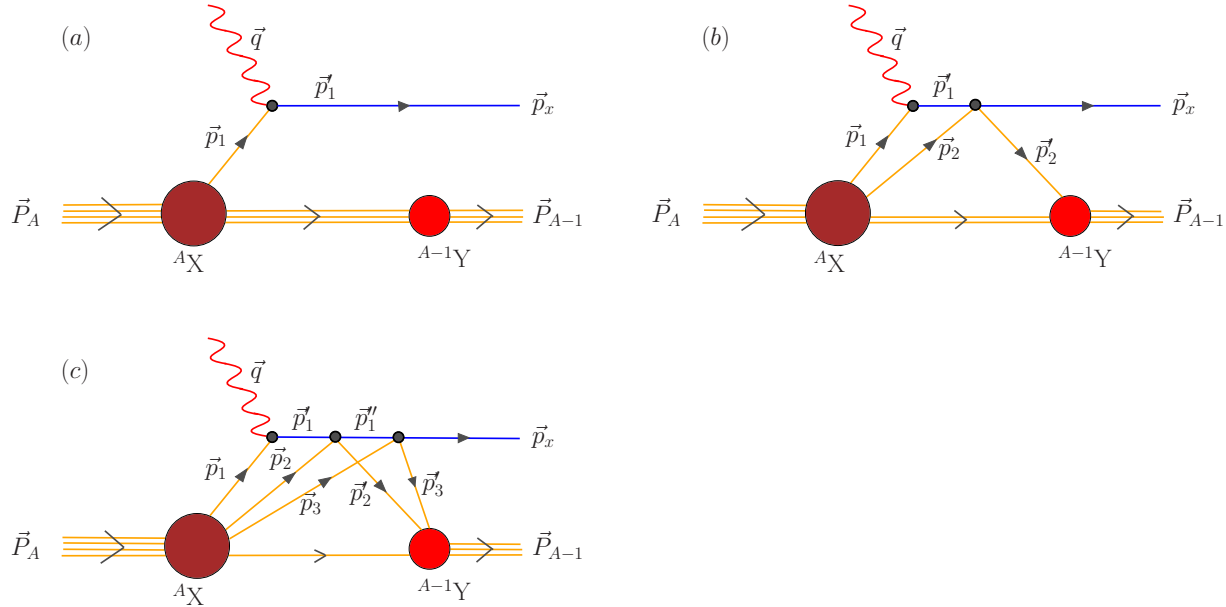


Figure 1. Feynman diagram vertex for a nucleon removal from the A_X nucleus. The free nucleon (a) does not interact with the nucleons (b) interacts with single nucleons and (c) interacts with pairs of nucleons, in the recoil nucleus $A-1_Y$.

3. Inclusive Electron-nucleus scattering

Consider an electron with an initial energy \mathcal{E}_i and momentum \vec{k}_i interacting with a nucleus with initial energy E_i and momentum \vec{P}_i . The electron transfers a photon of energy and momentum (ω, \vec{q}) to the nucleus and scatters with final energy and momentum $(\mathcal{E}_f, \vec{k}_f)$ at an angle θ_e . The final state of the nucleon system recoils with energy and momentum (E_f, \vec{P}_f) . In the case of a nucleon knock-out, the energy and momentum of the ejected nucleon are denoted by (E_x, \vec{p}_x) . The interaction of relativistic electrons with nuclei is well described by the impulse approximation.

The differential cross-section for inclusive electron-nucleus scattering, in the *one photon approximation*, is given by [1]

$$\frac{d^2\sigma}{d\mathcal{E}_f d\Omega_e} = \sigma_M \left[\left(\frac{Q^2}{q^2} \right)^2 R_L(\omega, \vec{q}) + \left(\frac{Q^2}{2q^2} + \tan^2 \frac{\theta_e}{2} \right) R_T(\omega, \vec{q}) \right] \quad (11)$$

where $Q^2 = q^2 - \omega^2$, σ_M is the Mott differential cross section and $R_L(\vec{q}, \omega)$ ($R_T(\vec{q}, \omega)$) the longitudinal (transverse) nuclear response function. The transverse response is given by

$$R_T(\vec{q}, \omega) = \frac{1}{2J_i + 1} \sum_f \left| \langle J_f^{\pi_f} M_f | \vec{j}_\perp(\vec{q}, \omega) | J_i^{\pi_i} M_i \rangle \right|^2 \delta(\omega - \Delta E) \quad (12)$$

where $|J_i^{\pi_i} M_i\rangle$ is the initial state of the target nucleus with parity π_i , angular momentum J_i , angular momentum projection M_i along the quantization axis, and $\vec{j}_\perp(\vec{q}, \omega)$ the components of the nuclear current operator that are perpendicular to \vec{q} . The coordinate system is oriented such that \vec{q} is directed along the z -axis, which is also chosen to be the quantization axis. For the function $R_L(\vec{q}, \omega)$ the nuclear charge operator $\rho(\vec{q}, \omega)$ is used in the place of $\vec{j}_\perp(\vec{q}, \omega)$. The delta function expresses the conservation of energy with $\Delta E = T_p + T_{A-1} + \Delta M$, where T_p (T_{A-1}) is the non-relativistic energy of the proton (recoil nucleus) and $\Delta M = M_A - M_{A-1} - M_x$ the separation energy of a proton (mass M_x) from the target nucleus (mass M_A). The nuclear charge and current operators used in this work are of the form [15]

$$\rho(\vec{q}, \omega) = \frac{q}{Q} G_E^x(Q^2) + \frac{i}{4M_x^2} \frac{2G_M^x(Q^2) - G_E^x(Q^2)}{\sqrt{1+\eta}} \vec{\sigma}_x \cdot \vec{q} \times \vec{p}_x \quad (13)$$

$$\vec{j}(\vec{q}, \omega) = \frac{\sqrt{\eta}}{q} \left[\left(2G_E^x(Q^2) + \eta G_M^x(Q^2) \right) \vec{p}_x - i G_M^x(Q^2) \left(\vec{q} \times \vec{\sigma}_x + \frac{\omega}{2M_x} \vec{q} \cdot \vec{\sigma}_x \vec{q} \times \vec{p}_x \right) \right] \quad (14)$$

where $\vec{\hat{q}} = \vec{q}/|\vec{q}|$, $\eta = Q^2/4M_x^2$ and G_E^x (G_M^x) the nucleon Sachs electric (magnetic) form factor. For the Sachs form factors the phenomenological parametrization derived in Ref. [16] is adopted.

4. The ${}^4\text{He}(e, e' p){}^3\text{H}$ reaction

The longitudinal and transverse response function for the inclusive ${}^4\text{He}(e, e' p){}^3\text{H}$ process are calculated for the kinematics of the experimental results presented in reference [17]. To evaluate the response functions it is convenient to decompose the initial state of the target in the form

$$|J_i^{\pi_i} M_i\rangle_A = \sum_{m_p} \langle j_p m_p J_o M_o | J_i M_i \rangle \left[|j_p^{\pi_p} m_p\rangle \otimes |J_o^{\pi_o} M_o\rangle_{A-1} \right] \quad (15)$$

where $|j_p^{\pi_p} m_p\rangle$ is the proton initial state and $\langle j_p m_p J_o M_o | J_i M_i \rangle$ Clebsch-Gordan coefficients. The theoretical results are compared with experimental data for $q = 300 \text{ MeV}/c$, $q = 400 \text{ MeV}/c$ and $q = 500 \text{ MeV}/c$ in figure 2. PWIA results are also shown and compared with the

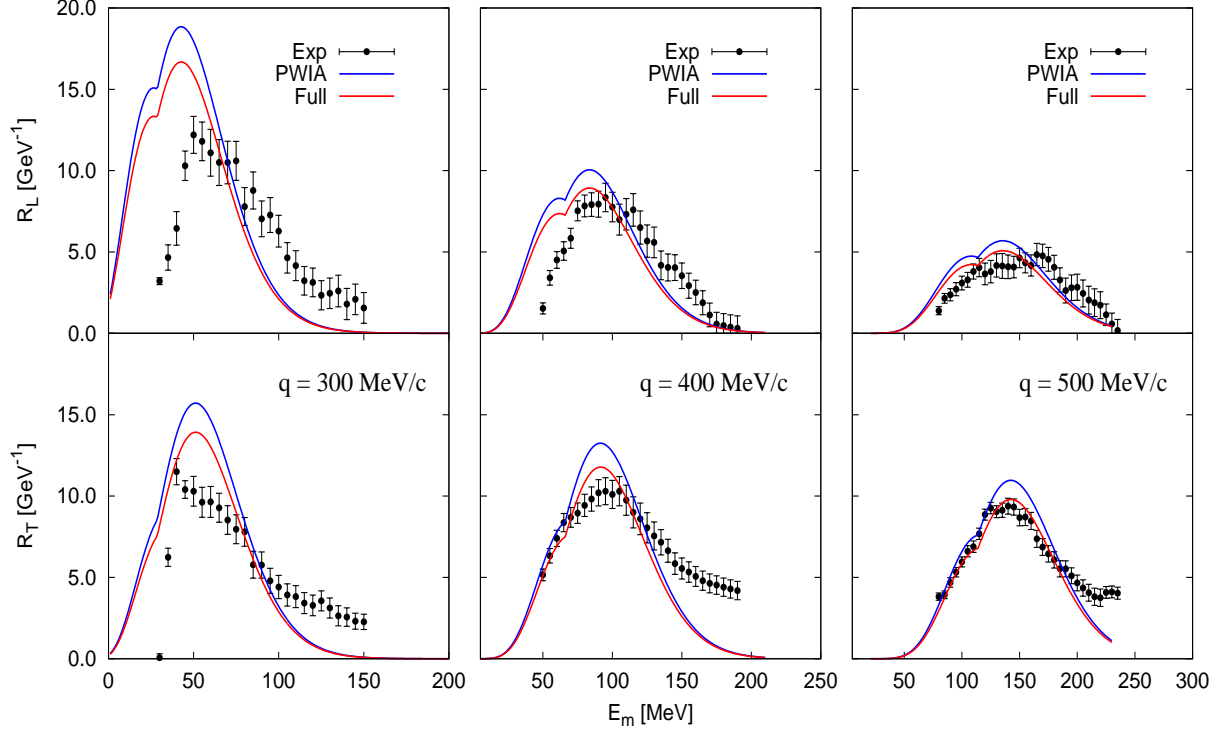


Figure 2. The longitudinal (R_L) and transverse (R_T) response function for the ${}^4\text{He}$ nucleus at $q = 400 \text{ MeV}/c$, $q = 400 \text{ MeV}/c$ and $q = 500 \text{ MeV}/c$. The experimental data are from reference [17].

results that include FSIs. The results of the longitudinal response function $R_L(\vec{q}, \omega)$ reproduce the general structure of the experimental data for all the values of q , with the size of the peak decreasing as q increases. For values of $E_m = \omega > 100 \text{ MeV}$ the theoretical results reproduce the experimental data satisfactorily. However, for $\omega < 100 \text{ MeV}$ the theoretical results overestimate the experimental data. The discrepancy between theory and experiment decreases as q increases. The contributions of the FSI to the theoretical response functions decrease the disparity between theory and experiment. The theoretical results for the transverse response functions $R_T(\vec{q}, \omega)$ overestimate the experimental data at low energy transfers. The transverse response is generally well predicted. The AMD results are consistent with the theoretical results presented in reference [17].

5. Conclusions

The AMD approach was used to investigate the electron-induced proton knock-out process in the ${}^4\text{He}$ nucleus. FSI between the ejected proton and the recoil nucleus are included using the Glauber approximation. Transverse and longitudinal response function the two-body electrodisintegration at high missing momenta were calculated. The AMD results gave a very good description of the experimental data. It was observed that the inclusion of FSI in general, improves the agreement between theory and experiment. Furthermore, the AMD results are consistent with results obtained using other theoretical methods. Therefore, AMD provide a simple yet accurate bound-state wave functions to of nuclear systems.

Acknowledgments

This work is part of a PhD thesis submitted to the University of South Africa.

References

- [1] Benhar O, Day D, Sick I, 2008 *Rev. Mod. Phys.* **80**, 189
- [2] Horiuchi H 1991 *Nucl. Phys.* **A 522** 257c
- [3] Caurier E, Grammaticos B and Sami T 1982 *Phys. Lett.* **B 109** 150
- [4] Feldmeier H 1990 *Nucl. Phys.* **A 515** 147
- [5] Ono A, Horiuchi H, Maruyama T and Ohnishi A 1992 *Prog. Theor. Phys.* **87** 1185
- [6] Tanaka E I, Ono A, Horiuchi H, Maruyama T and Engel A 1995 *Phys. Rev.* **C 52** 316
- [7] Togashi T, Katō K 2007 *Prog. Theor. Phys.* **117** 189
- [8] Watanabe T and Oryu S 2006 *Prog. Theor. Phys.* **116** 429
- [9] Kanada-En'yo Y, Horiuchi H and Ono A 1995 *Phys. Rev.* **C 52** 628
- [10] Peierls R E and Yoccoz J 1957 *Proc. Phys. Soc.* **A 70** 381
- [11] Wiringa R B and Pieper S C 2002 *Phys. Rev. Lett.* **89** 182501-1
- [12] Rampho G J 2011 *Few-Body Syst.*, **50**, 467
- [13] Rampho G J 2010 *PhD Thesis*, University of South Africa, unpublished.
- [14] Morita H, Ciofi degli Atti C, Treleani D 1999 *Phys. Rev.* **C60**, 034603-1
- [15] Schiavilla R, Benhar O, Kievsky A, Marcucci L E, Viviani M 2005 *Phys. Rev.* **C72**, 064003-1
- [16] Friedrich J and Walcher Th 2003 *Eur. Phys. J.* **A 17** 607
- [17] von Reden K F, *et al*, 1990 *Phys. Rev.* **C41**, 1084